*Materials Science-Poland, 36(2), 2018, pp. 225-234*
*http://www.materialsscience.pwr.wroc.pl/*
*DOI: 10.1515/msp-2018-0024*

**DE GRUYTER** OPEN

# Electron work functions of (h k l)-surfaces of W, Re, and Cu crystals

S.A. SURMA, J. BRONA*, A. CISZEWSKI

Institute of Experimental Physics, University of Wroclaw, Pl. Maxa Borna 9, 50-204 Wroclaw, Poland

Work function (WF) and some physicochemical data for several most prominent crystal planes of three metals of typical structures are calculated within the linear approximation employing the surface dipole and 2D gas models. "Composite" crystal of a homogeneous bulk phase and a thick surface composed of eight (h k l)-oriented facets with different unsaturated bonds is treated as a nine-phase nine-component system with two degrees of freedom. It contains the two-dimensional metal-lattice plasma of free electrons and the immobile atom-core network. For twenty four (h k l) surfaces, the WF and dipole barrier term, chemical and electrostatic potential levels, electron charge densities, surface dipole fields, and other parameters are calculated and tabularized. WF values obtained from the thermodynamics based formula are compared to the ones obtained from the quantum mechanics based formula, which shows good agreement with experiment and also reveals a specific deviation in the case of field emission method for the most packed plane. A set of accurate face dependent data can be of interest to electronics and materials science workers.

Keywords: *surface; interface; electron emission; work function; 2D plasma density; local Fermi levels*

## 1. Introduction

Electron work function (WF) is an important physicochemical characteristics of nanostructures, thin films, and solid metal or semiconductor surfaces [1–3]. The WF, or the smallest external energy loss required to transfer an electron from the crystal to the outside vacuum, depends on the electronic structure and crystallinity of the surface phase apart from the homogeneous bulk chemical potential. Bardeen [4], taking into consideration the electronic effects of exchange and correlation (XC), calculated the surface double layer (DL) moment as the WF contribution for a simple metal. Smoluchowski [5] considered the WF anisotropy as caused by the effects of the (h k l)-dependent electronic charge-density redistribution responsible for the existence of the negative DL moment as the resultant of two inverse surface dipole moments. His calculated differences of WF between the (h k l) surfaces of a bcc crystal decreased with decreasing atomic surface density and the relative surface energies increased in the same order. The order appeared to be quite a general qualitative criterion to check the face-dependent results for metals, which is known as the Smoluchowski rule. For the classical self-consistent calculation of the WF, Lang et al. [6, 7] used the surface dipole contribution and the jellium model. Boudreaux [8], in a quantum-mechanical attempt to calculate the one-electron potential energy functions, considered the potentials interactions of an electron with each lattice site rather than the jellium model.

Methfessel et al. [10] approached the face-dependent WF problem starting with Poisson equation and using the Hohenberg-Kohn DFT formalism [9] to treat the interacting inhomogeneous electron gas. Knapp [11] applied Herring-Nichols thermodynamics-based approach to WFs of (h k l) faces with the electrostatic patch fields. Wojciechowski et al. [12], Kiejna [13] employed the local metal-lattice plasma (MLP) polarization concept of Halas and Durakiewicz [14, 15] to calculate the face-dependent WF using the Kiejna self-consistent electron density profiles of stabilized jellium. Brodie et al. [16] proposed a general phenomenological model using the Maxwell classical image force and assuming Brodie minimum

*E-mail: jacek.brona@ifd.uni.wroc.pl

© 2018. This is an open access article distributed under the Creative Commons Attribution-NonCommercial-NoDerivatives 3.0 License. (http://creativecommons.org/licenses/by-nc-nd/3.0/)

uncertainty distance [17] for the surface 2D plasma, to cover both clean and electropositive adsorbate covered surfaces. An LEED experimental and theoretical study of the 1D surface-potential barrier for the W(1 1 0) and (1 0 0) surfaces was done by Baribeau et al. [18]. In their model, the potential-energy space was divided into three structural parts including the vacuum, and showed a distinct boundary between the surface skin (or selvedge) of 2 to 3 atomic layers and the volume structure.

Based on the Helmholtz 2D gas concept, the surface dipole barrier was related to MLP density fluctuations; many (h k l)-dependent WF values were computed for nine d transition metals by the linear regression method applied to a set of data from a great number of existing experimental WF values [19]. Employing the plasma polarization concept, we have presented an approximate formula for the WF by considering the total energy of a neutral two-component two-phase polycrystalline system of the 2D surface and 3D bulk [20]. Moreover, the semi-empirical expression for the screened electrostatic potential with its two extrema included both the effect of crystallinity and the XC effects.

In the present study, an attempt to resolve the face-dependent WF problem is made; the W, Re, and Cu metals have been chosen to represent three typical bcc, hcp and fcc structures. In contrast to our previous case with the interfaces of the undefined "polycrystalline" orientation [20], a set of eight atomically flat (h k l) surfaces of Me crystals has been taken into consideration to define the primary MLP parameters. The seven crystallographic planes of the conventional close-class [19] for each structure was defined in accord with the empirical relative prominence rule of face orientations that appear upon crystallization. The $d_s$(h k l) module, which is proportional to the scalar product of the surface normal multiplied by the primary bond vector [21], was treated as the local MLP characteristic dimension which determines the phase boundary position between an Me face and the bulk.

## 2. Basics

Procedures of crystallography based calculation and definitions of the parameters were previously described [20]. The calculations are continued in the system CGS ESU; units of (1 Å $= 1 \times 10^{-10}$ m, 1 eV $\approx 1.602 \times 10^{-19}$ J and 1 D (debye) $\approx 3.3356 \times 10^{-30}$ C·m) are also used. Potential energies are relative to the zero chosen at infinity in vacuum. The origin shift $x_0$ is taken equal to the polarization length L(h k l) of the low-temperature isothermal MLP and is calculated by using the electronic density $n_s$(h k l) of metal surface (MS) phases. The first geometrical plane is chosen as the origin of the coordinate system; the ideal physical surface location is ∼2 Å from it. Any (h k l)-oriented surface has the normal: (h k l) ≡ h; index h hereafter stands for (h k l). Parameters used to calculate the densities and MLP associated quantities are collected in Table 1.

The vacuum dielectric constant equal to unity was usually ascribed to metals. The MLP is treated as having the dielectric constant in the range of $0 < \epsilon \leqslant 1$. Like in the case of gas discharge plasma, enhancement of the inner electric field locally occurs in the DL rather than the dielectric-type reduction [22]. The effect is due to the leak of free electrons outside the outer atomic layers, which corresponds to the Smoluchowski electron cloud. The electronic MS consists of nondegenerate or thermalized electrons that are subject to the Maxwell-Boltzmann velocity distribution. The x-dependence of the electron electrostatic potential V has been expressed [20] by the set of equations:

$$\begin{aligned} V(x) &= \Phi_v && \text{for } x \leqslant -d_s \text{ in bulk phase,} \\ V(x) &= \Phi_s && \text{for } -d_s < x < x_l \text{ in surface phase,} \\ V(x) &= \Psi_c && \text{for } x \geqslant x_l \end{aligned} \tag{1}$$

where $x_l$ is the potential lacing point equal to $R_d - l_s/4$; $l_s$ is the dipole length attributed to the DL, and $2R_d$ is the mean size of a polarized MS atom.

To deal with the WFs we use a field-emitter-like model of a hemispherical crystal. Multifaceted body in the form of an h-oriented crystal with a finite curvature radius well reflects the difference in bonding between the bulk-lattice ions and the

Table 1. Face dependent metal-lattice plasma parameters for W, Re, and Cu.

| Tungsten[a,b]<br>rhenium[a,b]<br>copper[a] | (1 1 0)<br>(0 0 1)<br>(1 1 1) | (2 1 1)<br>(1 0 0)[d]<br>(1 0 0) | (1 0 0)<br>(1 0 1)[d]<br>(1 1 0) | (1 1 1)<br>(1 0 2)<br>(3 1 1) | (3 2 1)<br>(1 1 0)<br>(3 3 1) | (3 1 0)<br>(1 1 1)<br>(2 1 0) | (3 3 2)<br>(1 1 2)<br>(2 1 1) | (6 1 1)[c]<br>(1 1 4)[c]<br>(3 2 0)[c] | poly-crystal |
|---|---|---|---|---|---|---|---|---|---|
| Primitive unit cell area $S_{0,h}/a^2$ | $(\sqrt{2})/2$<br>$(\sqrt{3})/2$<br>$(\sqrt{3})/4$ | $(\sqrt{6})/2$<br>1.615<br>0.5 | 1<br>1.832<br>$(\sqrt{2})/2$ | $\sqrt{3}$<br>2.368<br>$(\sqrt{11})/4$ | $(\sqrt{14})/2$<br>2.797<br>$(\sqrt{19})/4$ | $(\sqrt{10})/2$<br>2.928<br>$(\sqrt{5})/2$ | $(\sqrt{22})/2$<br>3.289<br>$(\sqrt{6})/2$ | $(\sqrt{38})/2$<br>4.452<br>$(\sqrt{13})/2$ | 1.494<br>2.242<br>0.843 |
| MS thickness[e] $d_{s,h}$ [Å] | 2.238<br>2.228<br>2.087 | 2.584<br>2.390<br>1.808 | 1.583<br>2.106<br>2.556 | 2.741<br>2.445<br>2.180 | 2.538<br>2.760<br>2.488 | 2.002<br>2.636<br>2.425 | 2.699<br>2.347<br>2.214 | 2.054<br>2.601<br>2.507 | 2.737<br>2.950<br>2.685 |
| Polarization length[f] ($x_0$) $L_h^0$ [Å] | 0.434<br>0.427<br>0.410 | 0.502<br>0.487<br>0.393 | 0.370<br>0.472<br>0.481 | 0.542<br>0.524<br>0.466 | 0.535<br>0.561<br>0.512 | 0.471<br>0.557<br>0.510 | 0.568<br>0.545<br>0.501 | 0.534<br>0.595<br>0.558 | 0.529<br>0.553<br>0.503 |
| Effective dipole length $l_{s,h}$ [Å] | 0.1011<br>0.0738<br>0.099 | 0.1167<br>0.0791<br>0.0875 | 0.0715<br>0.0698<br>0.1236 | 0.1238<br>0.0810<br>0.1053 | 0.1147<br>0.0914<br>0.1204 | 0.0905<br>0.0873<br>0.1172 | 0.1219<br>0.0777<br>0.1071 | 0.0928<br>0.0861<br>0.1212 | 0.1283<br>0.0987<br>0.0657 |
| e-charge coverage $\theta_{s,h}$ | 0.6666<br>0.8130<br>0.8130 | 0.3846<br>0.4367<br>0.6757 | 0.3534<br>0.3774<br>0.4975 | 0.2717<br>0.2933<br>0.4167 | 0.2519<br>0.2519<br>0.3236 | 0.2604<br>0.2387<br>0.3115 | 0.2008<br>0.2101<br>0.2841 | 0.1335<br>0.1565<br>0.1938 | 0.303<br>0.311<br>0.413 |
| MS atomic density $n_{c,h}$ [$Å^{-3}$] | 0.0631[g]<br>0.0680[g]<br>0.0847[g] | 0.0315<br>0.0340<br>0.0847[g] | 0.0631[g]<br>0.0340<br>0.0423 | 0.0210<br>0.0227<br>0.0423 | 0.0210<br>0.0170<br>0.0282 | 0.0315<br>0.0170<br>0.0282 | 0.0158<br>0.0170<br>0.0282 | 0.0158<br>0.0113<br>0.0169 | 0.0244<br>0.0198<br>0.0338 |
| MS electronic density $n_{s,h}$ [$Å^{-3}$] | 0.1536[h]<br>0.1692<br>0.2155 | 0.0641<br>0.0766<br>0.2783 | 0.4010[i]<br>0.0928<br>0.0828 | 0.0402<br>0.0497<br>0.0996 | 0.0436<br>0.0327<br>0.0567 | 0.0932<br>0.0342<br>0.0582 | 0.0306<br>0.0393<br>0.0650 | 0.0443<br>0.0231<br>0.0337 | 0.0467<br>0.0359<br>0.0631 |
| Number of free electrons/atom $n_{c,h}/n_{s,h}$ | 0.41<br>0.40<br>0.39 | 0.49<br>0.44<br>0.30 | 0.16<br>0.37<br>0.51 | 0.52<br>0.46<br>0.42 | 0.48<br>0.52<br>0.50 | 0.34<br>0.50<br>0.48 | 0.52<br>0.43<br>0.43 | 0.36<br>0.49<br>0.50 | 0.52<br>0.55<br>0.54 |

[a]The first seven planes for each structure are those of the crystallographic close-class; for the planes' class discrimination [19].
[b]Using the linear regression constants by Surma [19], based on a large set of experimental data of the years: 1945 – 2000: $B^W = 1.34$ eVa, $A^W = 4.267$ eV; $B^{Re} = 1.085$ eVa, $A^{Re} = 4.736$ eV.
[c]One of the morphologically prominent crystallographic open-class planes.
[d]Calculated taking the high-coordination variant of surface structure.
[e]Computed using equation 2 by Surma [19].
[f]Computed using equation 5 by Surma et al. [20].
[g]Value coinciding with $\Omega^{-1}$.
[h]$\sim$0.1533 the free electron average density ñ.
[i]Same value was used for the polarizability in the Hohenberg-Kohn theory of inhomogeneous electron gas [9]. Note, their dielectric constant $\epsilon(\omega) > 1$ and tends to unity for large $\omega$.

surface-phase atoms. An instructive model of directional unsaturated surface bonds was proposed by Knor et al. [23]. A crystal of several h-oriented grains, which are ended with atomically flat surfaces, has a curved surface with a finite radius. Brodie, in his original model [16], has shown in fact that the sphere-symmetry WF practically corresponds to that of a planar system. Consequently, the MLP physicochemical system can comprise m independent species, and m phases (here, m = 9) in accord with the commonly accepted picture of the two-dimensional MLP. The arbitrarily chosen number nine covers the system's components of the free electron gas and eight surface-atom cores of different symmetry; the surface phases of the model crystal are eight facets of different symmetry each and the ambient vacuum. This is illustrated in Fig. 1.

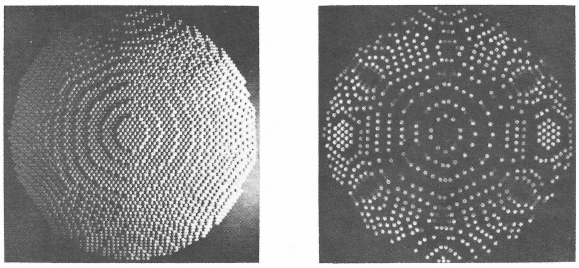

Fig. 1. Ball model of the nearly hemispherical multi-faceted field emitter tip of a bcc metal. The right-hand side picture shows edge atoms that most contribute to the field ion current. Taken from Mueller et al. [41]; courtesy of Professor T.T. Tsong, with permission by Elsevier.

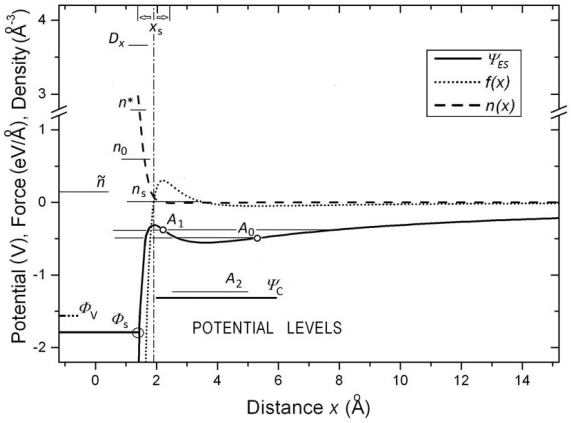


Fig. 2. The screened "double well" electrostatic potential $\Psi_{ES}$ with its first f(x) and second n(x) derivatives, and the inner potential levels $\Phi$. Small circles enclose inflexion points, larger circle indicates the potential lacing point at ~1.4 Å. Chain line $x_s$ shows the position of an ideal physical surface. Lines A show affinity levels; letters n indicate a conventional distribution of main electron number densities, $D_x$ denotes the normal field component; the MLP limiting density $n^* = 21.2 \times 10^{23}$ cm$^{-3}$. Diagram taken from Surma et al. [20].

## 2.1. Definition: inner potential $\Phi_{s,h}$

In the previous study [20], the inner electrostatic potential level $\Phi_s$ was applied to find the screened two-extremum potential $\Psi_{ES}$ shown in Fig. 2. The $\Phi_{s,h}$ is defined as the face dependent sum of the outer electrostatic (or Volta) potential level $\Psi_{c,h}$ and the surface potential change $\chi_{s,h}$:

$$\Phi_{s,h} = \Psi_{c,h} + \chi_{s,h} \tag{2}$$

In that study we dealt with a polycrystalline two-phase two-component system with its resultant surface dipole barrier. For the h-surfaces, we have started treating, for the first time, the WF problem from the Gibbs function defined as G = Nf(T,P) = Nμ. The chemical, or electrochemical [24], potential μ of free electrons can be identified with the thermodynamic (TD) potential of the Gibbs function per particle [25]. In terms of statistical physics, the sum $\mu^0$(T,P) + u(x,y,z) is constant at a constant temperature T in the presence of the field u with the degree of homogeneity −1. This is simply the case of the inner electrostatic potential. Consequently, for the local virtual Fermi levels, the relation:

$$\mu_{T,h} = \mu^0 + e\Phi_{s,h} \tag{3}$$

is constant in equilibrium [24–26]; relation 16 in the work by Surma et al. [20].

## 2.2. Assumption 1: division of the system into regions

The conducting system of interest can be divided into regions treated as TD open systems with their partial volumes $v_{s,h}$. Each of the single-crystal phases is treated as being in the TD quasi-equilibrium state. Each phase taken separately contains a 2D body of MLP ions and free electrons. Note that the Boltzmann factor kT of the two-dimensional plasma-energy scale is present both in the MLP statistics and the Fermi-Dirac distribution.

## 2.3. Assumption 2: the limiting point $x_{c,h}$ on the XC interactions

The face-dependent outer electrostatic potential $\Psi_{c,h}$, for a neutral crystal in the absence of applied field, can be calculated by summing δW the virtual, purely electrostatic works which are executed on a massless test particle of the charge e by infinitesimally slow bringing it in a quasi-static reversible process, from infinity in the vacuum, under action

of the long range image (Coulomb) force down to the position $x_{c,h}$ outside the Me surface. The works are associated with the infinitesimal drops in potential energy, $-\delta e\Psi_x$ each. In such a reversible process being a dense set of consecutive equilibrium states, the closest surface atom still retains its original screening; then the dipole repulsion together with the electron XC effects may be neglected at a distance from the geometrical surface. We assume the image force to be applicable safely down to a point $x_{c,h}$ equal to or higher than $d_{s,h} + x_0$. Then, the outer-potential levels $\Psi_{c,h}(x)$ are calculated by integration:

$$\Psi_{c,h} = \int_{\infty}^{x_{c,h}} \frac{-e}{4(x-x_0)^2}\, dx = -\Delta\Psi_{\infty,x} \qquad (4)$$

where $\Psi_{x=\infty} = 0$. For an h-oriented facet this gives $\Psi_{c,h} = -e/4d_{s,h}$. For $x < x_{c,h}$ the XC interactions cannot be ignored.

### 2.4. WF basic formulae

The quantum mechanics based definition of the WF was given by Wigner et al. [27] and reads as follows. The electron work function of a crystal, for an electron removed outside from the highest energy state of the neutral crystal, is the difference in energy between a lattice with N electrons and the lattice with $N - 1$ electrons, which equals $-\mu$, augmented by the minimum work $e\Delta\Phi_{s,h}$ required to transfer the electron across an h-facet to the vacuum:

$$WF^{QM} = e\Delta\Phi_{s,h} - \mu \qquad (5)$$

where the difference $\Delta\Phi_{s,h}$ equals $\Psi_{c,h} - \Phi_v$; the $\Psi_{c,h}$ equals $-e/4d_{s,h}$ (Assumption 2); e is the elementary charge; $\Phi_v$ is the average inner electrostatic potential of bulk Me, which was calculated from the dipole moment $p_0$ by Surma et al. [20]. The $\Delta\Phi_{s,h}$ is the resultant dipole barrier at an h-oriented MS/vacuum interface. Alternatively, according to the thermodynamics based WF formula of Herring and Nichols:

$$WF^{Td} = e\Psi_{c,h} - \mu_{T,h} \qquad (6)$$

where $\mu_{T,h}$ is the local Fermi level equal to $\mu^0 + e\Phi_{s,h}$, maximum WF is sometimes defined as the energy required to remove an electron of a metal from the Fermi level to a point at infinity in the vacuum [28], i.e. taking the value zero for the outer potential $\Psi_{c,h}$. The calculated potentials are collected in Table 2, where the WFs are compared to experimental $WF^X$ values.

## 3. Local electron number densities

MS parameters used to calculate electronic densities are presented below. The $d_{s,h}$ values are computed using the formula given by Surma et al. [20]. The MLP local surface dipole moment $p_{s,0}$ was introduced as the product:

$$el_{s,h} = \frac{Bd_{s,h}}{2\pi e} \qquad (7)$$

where B is the constant, numerically equal to the slope of linear regression [19]. The semi-empirical parameter $l_{s,h}$ for the h surfaces is the surface-dipole length of the DL moment p of the magnitude $\theta p_{s,0}$ where $\theta$ is the face-dependent surface-charge redistribution factor, or electron "coverage" factor. The product of the dipole length $l_s$ and the area $S_0$ of a 2D primitive unit cell of an MS was defined as the inverse of the unit electron density $n_0$ of the locally polarized 2D plasma. The intensive parameter $\tilde{n}$, or the density of free electrons, was defined as the reciprocal of the crystal volume per atom reduced by the conventional volume of a lattice ion itself, i.e. using the van der Waals-type correction:

$$\frac{1}{\tilde{n}} = \Omega - \frac{4}{3}\pi(R_a - l_d)^3 \qquad (8)$$

where $l_d$ is the face-dependent surface dipole half-length, $\Omega$ is the volume per atom of the crystal, and $R_a$ is the metallic radius of an atom.

Density parameter $n_c(d_{s,h})$ is defined as the reciprocal of the specific volume of the infinite DL space. It is associated with lattice points and corresponds to the number density of MS atomic cores:

$$\frac{1}{n_{c,h}} = S_h d_{s,h} \qquad (9)$$

Table 2. Calculated local electrostatic fields, potential energies and work function for (h k l) surfaces of W, Re, and Cu.

| Tungsten<br>rhenium<br>copper[a] | (1 1 0)<br>(0 0 1)<br>(1 1 1) | (2 1 1)<br>(1 0 0)<br>(1 0 0) | (1 0 0)<br>(1 0 1)<br>(1 1 0) | (1 1 1)<br>(1 0 2)<br>(3 1 1) | (3 2 1)<br>(1 1 0)<br>(3 3 1) | (3 1 0)<br>(1 1 1)<br>(2 1 0) | (3 3 2)<br>(1 1 2)<br>(2 1 1) | (6 1 1)<br>(1 1 4)<br>(3 2 0) | poly-crystal |
|---|---|---|---|---|---|---|---|---|---|
| Local virtual DL field $F_{v,h}$ [VÅ$^{(1}$] | 25.55<br>27.43<br>31.98 | 14.74<br>14.7<br>27.69 | 18.05<br>12.96<br>19.58 | 10.42<br>10.02<br>16.7 | 9.65<br>8.5<br>12.7 | 11.44<br>8.13<br>12.39 | 7.72<br>7.23<br>11.3 | 5.84<br>5.3<br>7.69 | 12.09<br>10.59<br>16.42 |
| DL potential change $\chi_{s,h}$ [V] | −1.722<br>−1.646<br>−1.328 | −0.662<br>−0.508<br>−0.83 | −0.456<br>−0.34<br>−0.61 | −0.351<br>−0.238<br>−0.37 | −0.279<br>−0.196<br>−0.25 | −0.269<br>−0.168<br>−0.228 | −0.189<br>−0.118<br>−0.174 | −0.073<br>−0.072<br>−0.092 | −0.470<br>−0.321<br>−0.446 |
| Outer potential $\Psi_{c,h}$ [V] | −1.61<br>−1.62<br>−1.73 | −1.39<br>−1.51<br>−1.99 | −2.28<br>−1.71<br>−1.41 | −1.31<br>−1.47<br>−1.65 | −1.42<br>−1.31<br>−1.45 | −1.80<br>−1.37<br>−1.49 | −1.33<br>−1.53<br>−1.63 | −1.75<br>−1.38<br>−1.44 | −1.315<br>−1.22<br>−1.34 |
| Inner potential $\Phi_{s,h}$ [V] | −3.33<br>−3.27<br>−3.06 | −2.05<br>−2.02<br>−2.82 | −2.74<br>−2.05<br>−2.02 | −1.66<br>−1.71<br>−2.02 | −1.70<br>−1.51<br>−1.70 | −2.07<br>−1.54<br>−1.72 | −1.52<br>−1.65<br>−1.80 | −1.82<br>−1.45<br>−1.53 | −1.785<br>−1.54<br>−1.79 |
| Local Fermi level[b] $\mu_{T,h}$ [eV] | −7.36<br>−6.19<br>−7.23 | −6.08<br>−6.59<br>−6.99 | −6.77<br>−6.62<br>−6.19 | −5.69<br>−6.28<br>−6.19 | −5.73<br>−6.08<br>−5.87 | −6.10<br>−6.11<br>−5.89 | −5.55<br>−6.22<br>−5.97 | −5.85<br>−6.02<br>−5.70 | −5.817<br>−6.11<br>−5.96 |
| local Fermi energy $E_h^F$ [eV] | 10.46<br>11.16<br>13.11 | 5.84<br>6.58<br>15.54 | 19.83<br>7.47<br>6.93 | 4.28<br>4.93<br>7.84 | 4.52<br>3.73<br>5.38 | 7.50<br>3.84<br>5.48 | 3.57<br>4.22<br>5.90 | 4.57<br>2.96<br>3.80 | 4.73<br>3.97<br>5.78 |
| Effective barrier $W_h^m$ [eV] | 17.82<br>17.35<br>20.34 | 11.92<br>13.17<br>22.53 | 26.60<br>14.09<br>13.12 | 9.97<br>11.21<br>14.03 | 10.25<br>9.81<br>11.25 | 13.60<br>9.95<br>11.37 | 9.12<br>10.44<br>11.87 | 10.42<br>8.98<br>9.50 | 10.55[c]<br>10.08<br>11.74 |
| Calculated TD-based WF $WF^{Td}$ [eV] | 5.75<br>4.57<br>5.50 | 4.69<br>5.08<br>5.00 | 4.49<br>4.91<br>4.78 | 4.38<br>4.81<br>4.54 | 4.31<br>4.77<br>4.42 | 4.30<br>4.74<br>4.40 | 4.22<br>4.69<br>4.34 | 4.10<br>4.64<br>4.26 | 4.50<br>4.89<br>4.62 |
| Calculated QM-based WF $WF^{QM}$ [eV] | 5.13<br>5.56<br>(5.06) | 4.60<br>4.99<br>(4.81) | 4.50<br>4.91<br>(4.70) | 4.44<br>4.85<br>(4.58) | 4.41<br>4.83<br>(4.52) | 4.40<br>4.82<br>(4.51) | 4.36<br>4.79<br>(4.48) | 4.30<br>4.77<br>(4.44) | 4.50<br>4.89<br>4.62 |
| Experimental[d] work function $WF^X$ [eV] | 5.25<br>5.53<br>4.98 | 4.71<br>5.10<br>4.59 | 4.63<br>5.04<br>4.48 | 4.47<br>–<br>– | –<br>4.80<br>– | 4.30<br>4.70<br>– | –<br>–<br>4.53 | 4.30<br>4.72<br>– | 4.54<br>5.0<br>4.65 |

[a]Cu data were recalculated in this paper using more experimental data [42–46] of four measurement methods. New linear regression constants $B^{Cu} = 0.612$ eVa and $A^{Cu} = 4.394$ eV.
[b]Computed from equation 3; value recognized as the electrochemical potential.
[c]This value being close to the Fermi energy $E^F_{(110)}$ agrees with most of theoretical data for tungsten.
[d]For tungsten, data come from [47–49]. For rhenium, they were selected from [19].

where $S_h$ is the area of a primitive unit cell of a surface. The associated local electron density $n_{s,h}$ is defined as the reciprocal of an MLP volume $v_h^0$:

$$\frac{1}{n_{s,h}} = v_h^0 \tag{10}$$

where $v_h^0$ equals $S_h R_{d,h}$ and the $R_{d,h}$ is:

$$R_{d,h} = d_{s,h} - R_a + l_d \tag{11}$$

Density $n_{s,h}$ represents the face-dependent concentration of MS thermalized electrons, which qualitatively reflects the local variation of the density of states. The local densities $n_{c,h}$ and $n_{s,h}$ are associated with respective volumes because the surface comprises up to three atomic layers. The ratio $n_{c,h}/n_{s,h}$ defines the average number of free electrons per atom in the local volumes $v_h^0$.

# 4. Selected applications

## 4.1. Intrinsic electric fields

The force $f_x$, normal to the surface and acting on an electron between two infinite planes at a short distance, slightly higher than $R_d$ from the geometrical plane, is expressed by the product $-eD_x$ (Fig. 2). The normal component is an analogue of the field displacement vector of a lattice plasma; it represents the effective field of an h-surface layer. The normal component $D_x$ of the effective field displacement vector D is ascribed to the local MLP polarization of the surface layer; its effective value equals $4\pi\bar{\sigma}$. The corresponding average surface potential level $\chi_s$ is then equal to $-4\pi\bar{\sigma}l$. The field strength component $D_x/\epsilon$ represents the virtual intrinsic field $F_v$ of the magnitude $4\pi\sigma$, and depicts the force acting along the polarized plasma medium. The charge distribution is discrete, and respective field components vary over the DL region like those of an electric dipole field.

Assuming the relation $D = \epsilon F$ valid for the MLP, we put $\epsilon = \theta$ which is a real number such that $0 < \theta \leqslant 1$, or the surface charge redistribution factor defined in Refs. [19] and [20]. The maximum virtual field $F_v$ component in the MS dipole approximation is given by:

$$F_v = \frac{4\pi\theta e}{\varepsilon S_0} = \frac{4\pi e}{S_0} \tag{12}$$

The continuous distribution of the surface charge density $\bar{\sigma}$ at the physical surface is approximated by the average density $\Delta q/\Delta S$ which can be expressed as the ratio $e\theta/S_0$; thus:

$$D_{x,h} = \frac{4\pi e\theta_{s,h}}{S_{0,h}} \tag{13}$$

where $\theta_{s,h}$ is the surface charge redistribution factor for an h-oriented surface. Accordingly, div D or $dD_{x,h}/dx$ equals $4\pi\bar{\rho}_s$, where the average density of electronic charge $\bar{\rho}_s$ equals $\Delta q_{s,h}/\Delta v_e$ which we approximate by $en_{s,h}$. The face dependent virtual fields are then calculated from the relation $\theta F_{v,h} = D_{x,h}$. Values of virtual field strengths are collected in Table 2.

## 4.2. Face-dependent dipole term of WF

DL of electrostatic charge is treated as composed of two discretely charged planes which are separated by a finite distance in the x-direction parallel to the normal dimension $d_{s,h}$ of the surface phase (i.e. the skin thickness), and infinite in the lateral y, z dimensions. The respective field components vary over the DL region like those of an electric dipole field. After the surface dipole approach [19] for the discrete charge distribution of locally polarized MLP, the normal component $D_{x,h}$ is treated as the DL field.

The surface potential levels $\chi_{s,h}$ within the Me/vacuum interface, between the two infinite DL planes y, z distant by $l_{s,h}$ and uniformly charged with the free charge density $\bar{\sigma}_s$, are given by the product $-D_{x,h}l_{s,h}$, or:

$$\chi_{s,h} = -4\pi\bar{\sigma}_s l_{s,h} \tag{14}$$

where the product $-\bar{\sigma}_s l_{s,h}$ represents the effective moment $M_{s,h}$; the resultant moment is the sum of potential difference originated from the positive charge density and that from the electronic-density redistribution [19].

$$\chi_{0,h} = -4\pi\bar{\sigma}_0 l_{s,h} \tag{15}$$

The effective surface potential $\chi_s$ and the virtual potential $\chi_0$ should fulfill the Poisson equation $\nabla^2\chi = -4\pi\rho$. The pseudo-permittivity $\epsilon$ is replaced with a factor $\theta$ being a real number such that $0 < \theta \leqslant 1$. Consequently, we are driving at the approximate relation:

$$\chi_s/\chi_0 \approx \bar{\rho}_s/\rho_0 = \tilde{n}/n_0 \leq \varepsilon = \theta \tag{16}$$

The inner-potential energy difference $e\Delta\varphi$ corresponds to the electrostatic part of the Gibbs free energy difference within the face-dependent unit volume $v_h^0$ of DL with its local virtual field $F_{v,h}$. Assuming that dielectric constant is independent of electric field, and using, for the h-surfaces, the well-known formula on the electrostatic energy, the face-dependent dipole energy can be expressed as:

$$\Delta G^0 = \varepsilon(F_{v,h})^2 v_h^0/8\pi = -2\pi e M_{s,h} \tag{17}$$

where $M_{s,h} = -\theta e l_{s,h}/S_h$; which appears to express the Helmholtz dipole. In such a way, this calculated energy-per-electron portion $\Delta G_0$, which is equal to the useful (or inner) work in the MLP system, represents the effective dipole barrier $e\Delta\Phi$, i.e. the dipole contribution to the WF.

### 4.3. Face-dependent Fermi energies and barriers of W, Re, Cu

The MS phase with the h-dependent set of unsaturated bonds [21], exhibits the well-known difference in chemical specificity between different surfaces of catalytic metals. Hence, for eight surface phases, the virtual Fermi energy levels $\mu_{T,h}(T,P)$ of MLP electrons will vary from plane to plane. In thermal equilibrium ($T_e \approx T_c$), the local polarization of the surface phase appears. The local Fermi kinetic energy $E_h^F$ of an electron and other Fermi energies are obtained from the classical Sommerfeld relation for the kinetic energy of free electron gas:

$$E_h^F = \frac{1}{2}\hbar^2 m^{-1}(3\pi^2 n_s)^{2/3} \tag{18}$$

These calculated face-dependent Fermi energies are shown in Table 2 including also potential energy barriers $Wm_h$.

The maximal kinetic energy W which is needed for emission of an electron being at rest in the metal can be determined by keeping the condition $m_e v_x^2/2 \geqslant W$, where $v_x$ is the x-component of the electron velocity. The $v_y$ and $v_z$ velocities are parallel to the surface and do not contribute to electron emission. For different crystallographic faces, this energy can be expressed by the formula:

$$W_h^m = E_h^F + WF_h^\infty \tag{19}$$

where $WF_h^\infty$, equal to $-\mu_{T,h}$, is the maximum planar WF measured from the Fermi level. Negative of these local maximum kinetic energies determines the respective conduction-band bottoms.

## 5. Discussion

### 5.1. Basic surface phase parameters

The $d_{s,h}$ quantity [19–21], which determines the phase boundary position, was calculated in the hard-sphere approximation. Homogeneous bulk Me phase was defined as the interior part of the crystal, where the surface dipole layer is absent, which occurs for $x \leqslant -d_{s,h}$. In contrast to purely crystallographic parameters, the $d_{s,h}$ is independent of the Miller indices parity because it is an atomic coordination-type function of the spacing between h planes. Therefore, it is dependent on the fine structure of the outer atomic monolayers. It accounts for a variety of the unsaturated surface bonds, i.e. the semi-directional or quasi-covalent physicochemical bonding at the h surfaces. The calculated numbers of free electrons per atom in local volumes do not exceed 0.55 for all the three of metals, which is in accord with the classical theory of conductivity. Worthy of mention is the polycrystalline electron potential $\Psi_{ES}$ which reveals a maximum and a minimum which are both located outside the geometrical surface [20]. Interestingly, it nearly coincides with the form of the Tavares-Prausnitz total perturbed hard-sphere potential [29].

The extrema-related inflexion points determine the affinity levels, and the ground state level $A_0$ is lower than these $\chi_{s,h}$ levels for more-open structure planes of W, Re, Cu. It should be the case of surface states; and the difference $A_1 - A_0$ is equal to a resonance energy of about 0.12 eV. In the linear approximation, the XC effects should vanish outside each (h k l)-oriented surface, practically from the distance $x_{c,h}$ close to the minimum of the $\Psi_{ES}(x)$, for which we have approximated the outer potential level $\Psi_c$. It is also interesting that a nano-surface phase with its normal dimension $d_{s,h}$ of few angstroms can be treated as a quantum well. A nano-surface phase of such a thickness clearly corresponds to the field-emitter tip ending of the minimum thickness d responsible for the photoelectron emission oscillations [30]. Other quantum size effects (quantum wells) were also observed experimentally [31–34].

### 5.2. The face-dependent WF data vs. experiment and theory

The calculated WF values in Table 2 agree well with the experimental results except for that,

the TD formula based WFs and the quantum-mechanics based ones differ in magnitude for the most packed plane of each metal. Such a deviation of experimental WF, resulting chiefly from the field emission method, is systematically observed in the literature; in the latter case for the W(1 1 0) face, the WFs exceed 6 eV. This anomalous feature of the W(1 1 0) surface was discussed by Plummer et al. [35]. The effect of the strong electric field on the WF of W(1 1 0) was explained by Smith [36] in a self-consistent investigation. As asserted by Young et al. [37], the densest packed plane (1 1 0) with its minimum surface free energy and the highest WF, is the most representative of physicochemical properties for bcc metals. In fact, the most packed planes have appeared to be critical for the best fit in the previous linear regression calculations for all the nine of d transition metals [19].

The face dependent WF correlates with the surface free energy and agrees well with theoretical [10, 38] and experimental values of WF and surface energy for bcc an fcc metals, which is in accord with the Smoluchowski rule. The correlation can be confirmed by the results on the crystallographic anisotropy of surface free energy in the literature [39, 40] and references therein. All values for W and Re are close to the thermionic emission data obtained by linear regression. Generality of Brodie, Chow and Yuan's phenomenological model is burdened by a deviation from the Smoluchowski rule, e.g. for tungsten and silver facets [17]. Their general WF model, however, includes electropositive adsorbates on clean metals and oxides. To conclude, dipole models based results seem to be most proper for clean metals.

The calculated potential energy functions include the XC or polarization effects, which is in accord with the Boudreaux assertion [8]. The inner electrostatic potential of bulk Me, $\Phi_v$, was expressed in the previous study as an average of $(\Phi_{MS} + \Psi_{MS})/2$. Validity of such approximation of the potential difference was shown by Knapp for the mean WF [11], which was extended in his argumentation for the WF of an i-th face of a crystal with its i-th patch field. The $WF^{Td}$ of equation 6 is in accord with Knapp argumentation for the face dependent WFs.

## 6. Conclusion

The model of a "composite" metal similar to the multifaceted field emitter enabled us to compute work function values for the chosen metals of three main structures, for 24 different faces in total. The accuracy of the predicted values is estimated to be $\pm 0.1$ eV. They are in accord with available experimental values. Two WF formulae were used for comparison of the computed values, of which the thermodynamics based one better corresponds to the experimental values obtained by the FE method, especially in case of the W(1 1 0) face.

Two discontinuous quantities: the local Fermi levels $\mu_{T,h}$ of an electron and the electronic number densities $n_{s,h}$, which jump at each interface, are intensive parameters. In the limiting case, the electron density of the lattice plasma may reach a figure of $21 \times 10^{23}$ cm$^{-3}$, which is only fifty times lower than the maximum laboratory obtainable density of inertial confinement plasma. Virtual electrostatic fields related to the metal-lattice plasma are calculated to spread up to as high as about 32 V/Å (Cu(1 1 1)), whereas the typical field evaporation field intensities range from 3 to 6 V/Å for metals [41].

## References


[1] Herring C., Nichols M.H., *Rev. Mod. Phys.,* 21 (1949), 185.
[2] Kiejna A., Wojciechowski K.F., *Metal Surface Electron Physics,* Pergamon, Oxford, 1996.
[3] Halas S., *Mater. Sci.-Poland,* 24 (2006), 951.
[4] Bardeen J., *Phys. Rev.,* 49 (1936), 653.
[5] Smoluchowski R., *Phys. Rev.,* 60 (1941), 661.
[6] Lang N.D., Kohn W., *Phys. Rev. B,* 1 (1970), 4555.
[7] Lang N.D., Kohn W., *Phys. Rev. B,* 3 (1971), 1215.
[8] Boudreaux D.S., *Phys. Rev. B,* 1 (1970), 4552.
[9] Hohenberg P., Kohn W., *Phys. Rev.*, 136, B864 (1964).
[10] Methfessel M., Hennig D., Scheffler M., *Phys. Rev. B*, 46 (1992), 4816.
[11] Knapp A.G., *Surface Sci.*, 34 (1973), 289.
[12] Wojciechowski K.F., Kiejna A., Bogdanów H., *Modern Phys. Lett. B,* 13 (1999), 1081.
[13] Kiejna A., *Phys. Rev. B,* 47 (1993), 7361.
[14] Halas S., Durakiewicz T., *J. Phys.-Condens. Mater.,* 10 (1998), 10815.
[15] Durakiewicz T., Halas S., Arko A., Joyce J.J., Moore D.P., *Phys. Rev. B,* 64 (2001), 045101.

[16] BRODIE I., CHOW S.H., YUAN H., *Surface Sci.,* 625 (2014), 112.
[17] BRODIE I., *Phys. Rev. B*, 51 (1995), 13660.
[18] BARIBEAU J-M., LOPEZ J., LE BOSSE J.-C., *J. Phys. C-Solid State Phys.,* 18 (1985), 3083.
[19] SURMA S.A., *Phys. Status Solidi A,* 183 (2001), 307.
[20] SURMA S.A., BRONA J., CISZEWSKI A., *Mater. Sci.-Poland,* 33 (2015), 430.
[21] MACKENZIE J.K., MOORE A.J.W., NICHOLAS J.F., *J. Phys. Chem. Solids*, 23 (1962), 185.
[22] ARTSIMOVICH L.A., *Elementarnaya fizika plazmy,* Atomizdat, Moscow, 1969.
[23] KNOR Z., MÜLLER E.W., *Surface Sci.,* 10 (1968), 21.
[24] GUGGENHEIM E.A., *Thermodynamics,* North-Holland Elsevier, Amsterdam, 1993.
[25] LANDAU L.D., LIFSHITS E.M., *Statistical Physics,* Pergamon, London, 1980.
[26] KORYTA J., DVORAK J., BOHACKOVA V., *Lehrbuch der Elektrochemie,* Springer, Wien/NewYork, 1975.
[27] WIGNER E.P., BARDEEN J., *Phys. Rev.,* 48 (1935), 84.
[28] SCHULTE F.K., *J. Phys. C-Solid State Phys.* 7 (1974), L370.
[29] TAVARES F W., PRAUSNITZ J.M., *Colloid. Polym. Sci.,* 282 (2004), 620.
[30] RADOŃ T., *Acta Phys. Polon. A,* 118, (2010), 596.
[31] CHEN Y., ZHAO C., HUANG F., ZHAN R., DENG S., XU N., CHEN J., *Sci. Rep.,* 6 (2016), 21270.
[32] WOJCIECHOWSKI K.F., *Phys. Rev. B,* 60 (1999), 9202.
[33] HERMAN M.H., TSONG T.T., *Phys. Rev. Lett.,* 48 (1982), 1029.
[34] TOMASZEWSKI P.E., *Ferroelectrics,* 375 (2008), 74.
[35] PLUMMER E.W., RHODIN T.N., *J. Chem. Phys.,* 49 (1968), 3479.
[36] SMITH J.R., *Phys. Rev. Lett.,* 25 (1970), 1023.
[37] YOUNG R.D., CLARK H.E., *Phys. Rev. Lett.,* 17 (1966), 351.
[38] SKRIVER H.L., ROSENGAARD N.M., *Phys. Rev. B*, 46 (1992), 7157.
[39] DRECHSLER M., *The Equilibrium Shape of Metal Crystals,* in: VU T.B. (Ed.), *Surface Mobilities on Solid Materials,* Plenum Press, New York/London, 1983, pp. 405 – 457.
[40] KERN R., *The Equilibrium Form of a Crystal*, in: SUNAGAWA I. (Ed.), *Morphology of Crystals*, Terrapub, Tokyo, 1987, pp. 77 – 206.
[41] MUELLER E.W., TSONG T.T., *Field Ion Microscopy – Principles and Applications,* American Elsevier, New York, 1969, p. 70.
[42] LI D.Y., LI W., *Appl. Phys. Lett.,* 79 (2001), 4337.
[43] HAAS G.A., THOMAS R.E., *J. Appl. Phys.,* 48 (1977), 86.
[44] ROWE J.E., SMITH N.V., *Phys. Rev. B,* 10 (1974), 3207.
[45] GARTLAND P.O., BERGE S., SLAGSVOLD B.J., *Phys. Rev. Lett.,* 28 (1972), 738.
[46] DELCHAR T.A., *Surf. Sci.,* 27 (1971), 11.
[47] MICHAELSON H.B., *J. Appl. Phys.,* 48 (1977), 4729.
[48] FOMENKO V.S., PODCHERNYAEVA I.A., *Emissionnye i Adsorbtsionnye Svoistva Veshchestv i Materialov*, Atomizdat, Moscow, 1975.
[49] HAAS G.A., THOMAS R.E., *J. Appl. Phys.,* 40 (1969), 3919.

*Received 2017-11-15*
*Accepted 2018-02-15*